Wideband Analysis of Large Scale and Small Scale Fading in Tunnels

J.-M. Molina-Garcia-Pardo, M. Lienard, A. Nasr and P. Degauque, *Member, IEEE*

***Abstract*— In this contribution, the analysis and the modeling of the large scale and small scale fading statistics in a semicircular tunnel is presented. The results are based on experimental data obtained during an extensive measurement campaign in the 2.8 - 5 GHz frequency range. Lastly, a simple model to characterize the statistics of the received signal in tunnels is presented.**

I. Introduction

WIRELESS communications in confined environments, such as tunnels, have been widely studied for years, and a lot of experimental results have been presented in the literature, mainly to describe mean path loss versus frequency in environments ranging from mine galleries and underground old quarries to road and railway tunnels [1], [2].

Nowadays, Ultrawideband (UWB) approaches seem to be an interesting solution for providing high data rate communication. These UWB signals are characterized by a very large bandwidth, equal or greater than either 20% of the central frequency or than 500MHz. The main applications of this technique are UWB radars [3] and wireless communication systems [4]. In [5], and in [6], a complete state of the art of UWB is presented, ranging from the theory of the wireless channel, measurements and channel modeling.

Possible applications of UWB techniques for communications in transportation systems usually concern in-vehicle links. However, this technique is also a potential candidate to ensure vehicle to vehicle or vehicle to roadside communications. In a related domain, there is a special interest for increasing the data rate of train to train and train to track communications, by simultaneously ensuring distance measurements [7]. Since subways are often situated in an underground environment, UWB links in tunnel must be carefully studied. However, for the time being, there is a lack of experimental data dealing with wide band propagation characteristics in such an environment. The objective of this work is to fill this gap by investigating the behavior and the statistics of the electric field in a frequency range extending from 2.8 GHz to 5 GHz. Results focus on large scale fading and small scale fading, while statistical models, fitting the experimental data are also proposed.

The different sections of this paper are as follow: in section II we describe the geometrical environment and the procedure that has been followed to perform the measurement. Section III and IV investigate the distribution of the large scale fading and small scale fading, respectively. Finally section V summarizes the works.

II. Environment, Measurement Equipment and Methodolody

A. Description of the environment

The measurement campaign was performed in the tunnel of Roux, which is situated in the Ardèche region (central French mountain). This tunnel is perfectly straight and has a length of 3336 m. The transverse section of the tunnel is semicircular and has a diameter of 8.6 m. The maximum height is 6.1m at the centre of the tunnel (Fig.1).

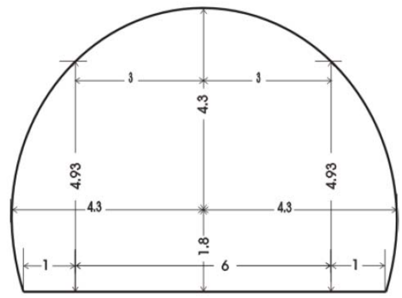

Fig. 1 Transverse plane of the tunnel.

B. Measurement Equipment

The measurement procedure is nearly the same as the one described in [8]. A network analyzer (Agilent E5071B) has been used to measure the radio channel frequency response, both in amplitude and phase. One port is used in transmission mode to generate a RF (Radiofrequency) signal which is converted to an optical signal and sent through fibre optics in order to avoid signal attenuation. Indeed, since distances up to 500 m are considered, the attenuation in coaxial cables is prohibitive. Then, the signal is converted

J.-M. Molina-Garcia-Pardo is with the Technical University of Cartagena, Departamento Tecnologías de la Información y las Comunicaciones Antiguo Cuartel de Antigones. Plaza del Hospital, 1. Campus Muralla del Mar, Universidad Politécnica de Cartagena 30202 Cartagena, Spain (Spain). (Telephone: +34 968 325363, Fax: +34 968 325973 Email: josemaria.molina@upct.es).

M. Lienard, A. Nasr and P. Degauque are with the University of Lille, IEMN / TELICE Lab., University of Lille, France, martine.lienard@univ-lille1.fr. This work has been supported by the European FEDER funds, the Region Nord Pas de Calais and the French Ministry of Research in the frame of the CISIT project on innovation in Transportation Systems.

978-1-4244-2858-8/08/$25.00 ©2008 IEEE

back to RF., amplified using two 30 dB amplifier and feeds a wideband antenna.

At the reception side, the receiving antenna is connected to the other port of the analyzer with a coaxial cable, few meters long. The complex channel transfer function is given by the S_{21} parameter. During the measurements, the tunnel is closed to traffic and the channel can be considered as stationary.

Two omnidirectional antennas (EM-6116) having an almost flat frequency response from 2 GHz up to 10 GHz have been used. Nevertheless, in order to be able to subtract the possible antenna effects in the measurements (this will be discussed in the next section), a reference case was considered by measuring the frequency response of the two antennas in an anechoic chamber. In this case, the two antennas are aligned in such a way that they transmit/receive in their main radiation lobes. It must be emphasized that change of the radiation pattern with frequency is not critical since, in tunnels, the main contribution to the received power comes from rays propagating nearly parallel to the tunnel axis, i.e. impinging the tunnel walls with a grazing angle of incidence.

In order to increase the number of measurement points, the channel response was measured by using two virtual arrays: one at the transmission site and another at the reception site. The antennas are put on a rail, 1.5 m long and placed perpendicular to the tunnel axis. A mechanical positioning system moves the antennas along this rail, the minimum step being equal to 1mm.

The block diagram of the channel sounder is depicted in Fig. 2.

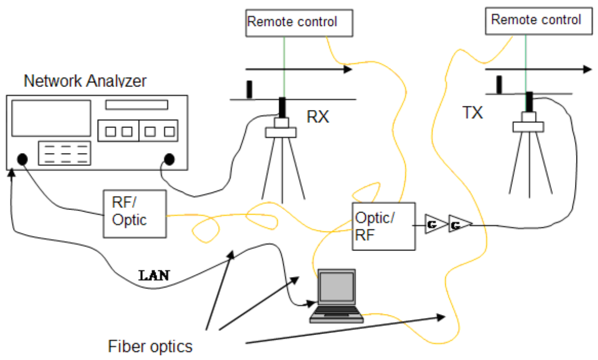

Fig. 2 Channel Sounder set-up.

C. *Methodology*

The channel response has been measured for 1601 frequency points, equally spaced in the range 2.8 GHz - 5 GHz. The intermediate frequency was 10 kHz and the radiated power 10 dBm. With this configuration, a dynamic range greater than 100 dB is obtained.

During the measurements, the transmitter and the receiver have been positioned on the same lane (the tunnel has two lanes, 4 meter each), and the distance between transmitter and receiver varies from 50m to 500m, with a 5m step. In the transverse plane, at any longitudinal distance, 12 successive positions for the transmitting antenna and for the receiving antenna were considered, using the rail and the mechanical system previously mentioned. The transverse step is 3cm (λ/2 at 5 GHz).

Fig. 3 summarizes the measurement scheme that we have followed.

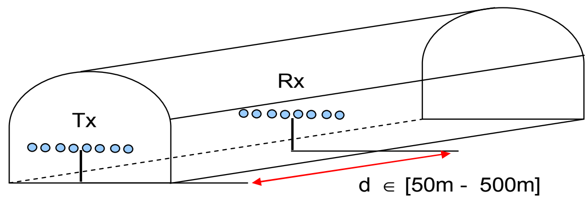

Fig. 3 Configuration of the wideband measurements.

III. Large Scale Fading

The path loss at each frequency, corresponding to the relative received power (the power in dB normalized to an input power of 0dB) is easily deduced from the S_{21} parameter:

$$\Pr(f) = 20 \cdot \log_{10}\left(\left|S_{21}(f)\right|\right) \qquad (1)$$

The relative received powers at 50m and 500m versus frequency are plotted in Figs. 4 and 5, respectively. The calibration of the network analyzer is made between the two points corresponding to the connection points of the transmitting and receiving antennas. Consequently, the effects of cables, connectors, amplifiers and optical transducers are eliminated but not those of the antennas.

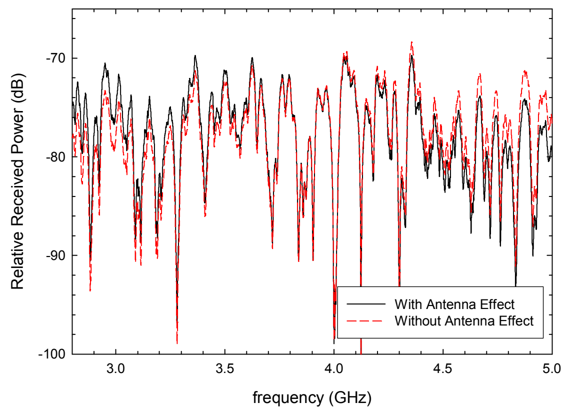

Fig. 4 Relative received power at 50m.

From preliminary measurements in an anechoic chamber, the variation of the antenna gain versus frequency can be subtracted, leading to the curves noted “without antenna effect” in Figs 4 and 5. Since, as we have already mentioned, the antenna gain is nearly flat in the frequency band under consideration, the curves with and without antenna effects are nearly the same.

To separate the large scale fading from the small scale fading, it is necessary to average the power received in a certain area. It is also possible to average in frequency as long as the selected bandwidth remains lower than the channel coherence bandwidth. In the case of this tunnel, a

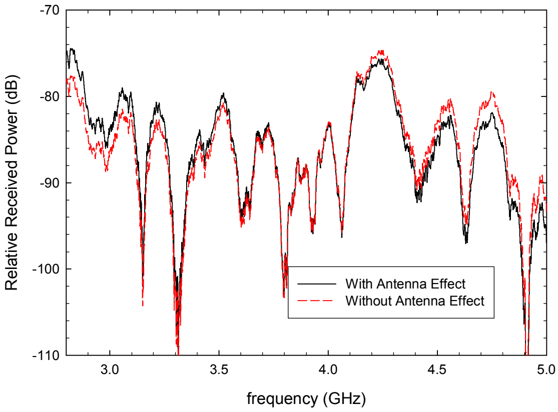

Fig. 5 Relative received power at 500m.

10MHz coherence bandwidth is obtained. Since the frequency step for each measurement is 1.4 MHz, one can average, for each longitudinal distance, on 7 successive frequencies and on the 12x12, i.e. 144 positions of the antennas in the transverse plane.

The averaged path loss (*PL*) is thus given by:

$$PL(f) = -20 \cdot \log_{10} \left\langle \left(S_{21} \right)_{(f \pm 5MHz, n, m)} \right\rangle \qquad (3)$$

Fig. 6 shows the variation of this path loss at 3GHz and 5GHz, the effect of the antennas being subtracted.

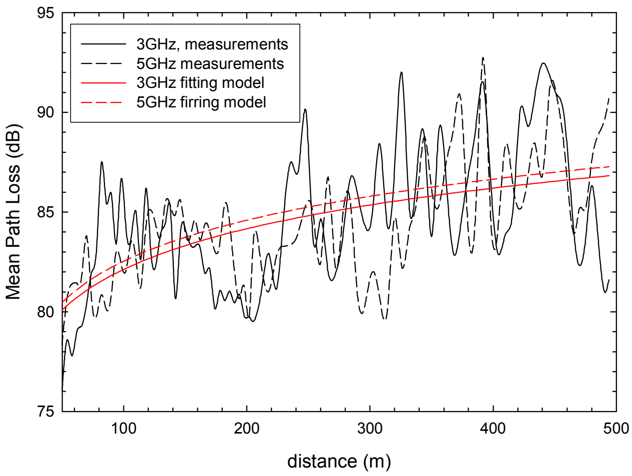

Fig. 6 Mean Path Loss versus longitudinal distance for two different center frequencies

In the literature, simple empirical equations are often proposed to predict the mean *PL* as a function of frequency and distance. Let us start from the following equation:

$$L = \left(L_0 + 10 \cdot n_{L_0} \log_{10} \left(f(GHz) \right) \right) + 10 n \log_{10}(d) + X_\sigma \qquad (4)$$

All parameters have to be evaluated so that the resulting curve *L* versus distance and/or frequency fits quite well the experimental results. Using an iterative procedure, the parameters minimizing the mean square error are given in Table I.

Parameters	L_0	n_{L_0}	n	σ
	68 dB	0.82	0.57	2.7 dB

Table I: Parameters for the mean path loss model in (4).

In order to compare our results to those found in the literature for other configurations, Table II, extracted from [9], gives the measured path loss exponents and shadowing standard deviation.

Researchers	*n* : Mean	*n* : Std. Dev.	σ (dB) : Mean	σ (dB) : Std. Dev.	Distance (m)
Virginia Tech (office) AT&T (Res.) [3]	1.3-1.4 (LOS) 2.3-2.4 (NLOS) 1.7 /3.5 (LOS/NLOS)	0.3 /0.97	2.5-3 (LOS) 2.6-5.6 (NLOS) 1.6/2.7	0.5/0.98	5-49 (LOS) 2-9 (NLOS) 1-15 (LOS) 1-15 (NLOS)
U.C.A.N. [8]	1.4/3.2(soft)/4.1(hard) LOS/NLOS/NLOS		0.35 LOS/1.21(soft) /1.87(hard) NLOS		4-14 (LOS/NLOS)
France Telecom [11] CEA-LETI [10]	1.5 / 2.5 (LOS/NLOS) 1.6 (lab)1.7(flat) LOS 3.7 (office/lab/NLOS) 5.1 (flat/NLOS)		4 / 4 (LOS/NLOS)		2.5-14 (LOS) 4-16 (NLOS) 1-6, 1-8 (LOS 2-20,7-17 (NLOS)
Intel [4](Resident.)	1.7/4.1 (LOS/NLOS)		1.5/3.6 (LOS/NLOS)		1-11 (LOS) 4-15 (NLOS)
IKT, ETH Zurich [13]	2.7- 3.3 (on body) 4.1 (around the torso)				0.15 – 1.05
Cassioli/ Molisch/Win [7]	2.04 (d<11m) -56+74log(d) (d>11)		4.3		8-11 (NLOS) 11-13(NLOS)
Oulu Univ. [9]	1.04,1.4,1.8 LOS 3.2, 3.3, 3.9 NLOS				1-30 (LOS) 4-14 (NLOS)
Whyless [5]	1.58/1.96 LOS/NLOS				2.5-16 (LOS/NLOS)
Time Domain [6]	2.1 (LOS/NLOS)		3.6		2-21 (LOS/NLOS)

Table II Measured Path Loss Exponents (n) and Shadowing Standard Deviation (σ) extracted from [9]

IV. SMALL SCALE FADING

Once the mean path loss is known, the small scale fading must be analyzed. Following the same procedure as previously, the field amplitude distribution at a given longitudinal distance, has been studied in a 10 MHz band and for the 144 positions of the antennas in the transverse plane. We have fitted the measured data to a Rayleigh, Weibul, Rician, Nakagami and Lognormal distribution, and then we have used the Kolmogorov-Smirnov test in order to decide what distribution fits the best the measurement results.

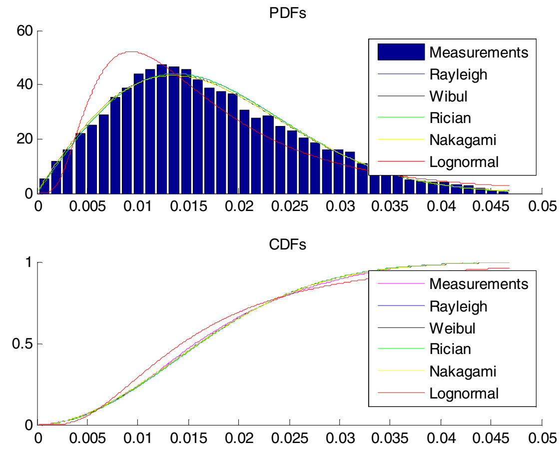

Fig. 7 Measured data and fitted distributions for a position at 50m and at 5GHz.

Fig. 7 shows the Probability Density Functions (PDFs) and the Cumulative Density Functions of the raw data and of the fitted models for a distance of 50m. We find that both

Weibul and Rice fit quite well the measurement statistics. In the following, we have preferred to choose the Rice distribution since it is widely used in telecommunications. The same approach has been made for other longitudinal distances, i.e. between 50m and 500m.

The PDF of a rician distribution is given by the following expression:

$$f(x \mid v,\sigma) = \frac{x}{\sigma^2} \exp\left(\frac{-(x^2+v^2)}{2\sigma^2}\right) I_0\left(\frac{xv}{\sigma^2}\right) \quad (5)$$

where $I_0(\ )$ is the modified Bessel function of the first kind of zero order. For such a distribution, the K factor, defined as the ratio between the deterministic component and the random component, can be easily deduced from the measurements of the complex value of the S_{21} parameter.

$$K = \frac{\text{Power of Constant Part}}{\text{Power of Random Part}} = \frac{\left|\langle S_{21}\rangle\right|^2}{\left\langle \left|S_{21} - \langle S_{21}\rangle\right|^2 \right\rangle} \quad (6)$$

where $\langle\ \rangle$ means averaging over all realizations.

By following the same approach as in the previous section, thus by averaging over 144 transverse positions and 7 frequencies, the K factor has been plotted in dB for three different center frequencies (Fig. 8).

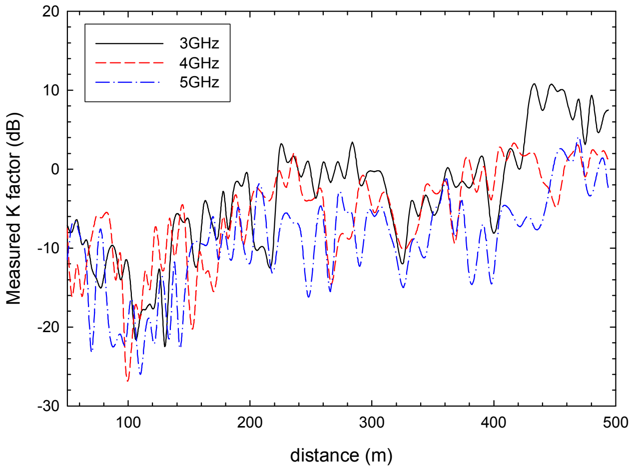

Fig. 8 K factor versus distance for three different frequencies.

We note that K is a continuously increasing function with distance. Furthermore, in average, this increase is slightly higher at 5 GHz than at 3 GHz. This can be explained by the number of propagating modes which depends both on frequency and on the longitudinal distance. To predict the K factor, one can use a simple empirical formula assuming a linear variation in dB with distance. The various parameters have been found by minimizing the mean square error.

Knowing K and by normalizing the average field amplitude to 1, the parameters s and σ of the Rice distribution can be deduced from (7):

$$\left.\begin{aligned} E(X) &= \sqrt{\frac{\pi}{2}}\,|\sigma|\,L_{1/2}\left(-\frac{s^2}{2\sigma^2}\right) = 1 \\ K &= \frac{s^2}{2\sigma^2} \end{aligned}\right\} \begin{aligned} |s| &= \sqrt{2K|\sigma|^2} \\ |\sigma| &= \sqrt{\frac{2}{\pi}}\frac{1}{L_{1/2}\left(-\frac{s^2}{2\sigma^2}\right)} \end{aligned} \quad (7)$$

The small scale variation of the phase of the S_{21} parameter has also been studied. To only mention one result, at large longitudinal distance, beyond 200m, the phase variation in the transverse plane at 3 GHz and at 5GHz are, in average, less than 0.8 radians and 2 radians respectively, for two points 0.33 cm apart. This leads to high correlated fields.

V. Conclusion

We have presented the analysis of the large scale and small scale parameters deduced from measurements performed in a straight semicircular tunnel in the 2.8GHz-5GHz bandwidth. In the case of the large scale fading, if the antenna gain is subtracted from the measurements, no significant attenuation is observed with frequency.

Regarding the small scale fading, a Rice distribution fits quite well the measurements. For the phase of the electric field in the transverse plane, a uniform distribution is found, with a range of values that decreases with longitudinal distance and increases with frequency.

In all cases, simple models are proposed to predict all these parameters, in order to develop a complete UWB channel model. Further works include the analysis of spatial and temporal correlation in order to construct a complete UWB-MIMO channel model.

References

[1] M. Liénard and P. Degauque, “Natural Wave Propagation in Mine Environments”, IEEE Transactions on Antennas and Propagation, vol. 48, no. 9, pp. 1326-1339, September 2000 .

[2] M. Lienard, P. Degauque, “Propagation in wide tunnels at 2 GHz: a statistical analysis”, Vehicular Technology, IEEE Transactions on vol. 47, pp:1322 – 1328, Nov. 1998.

[3] J. D. Taylor, Ed., *Introduction to Ultra-Wideband Radar Systems*, 1st ed.. Boca Ranton, FL: CRC Press, 1995.

[4] R. C. Qiu, H. Liu, and X. Shen, “Ultra-wideband for multiple access communications,” *IEEE Commun. Mag.*, vol. 43, pp. 80–87, 2005.

[5] A. F. Molisch, ”Ultrawideband Propagation Channels-Theory, Measurement, and Modeling”, *IEEE Transactions on Vehicular Technology,* vol. 54, no. 5, pp. 1528-1545, September 2005.

[6] A. F. Molisch, “Ultrawideband propagation channels and their impact on system design”, International Symposium on Microwave, Antenna, Propagation and EMC Technologies for Wireless Communications, page(s): K4- 1-K4- 5, 16-17 Aug. 2007

[7] H. Saghir, M. Heddebaut, F. Elbahhar and J.M. Rouvaen, “Evaluation of a Tunnel Ground to Train UWB Communication”, IEEE 64th Vehicular Technology Conference, pp. 1-5, September 2006.

[8] J.-M. Molina-García-Pardo, J.-V. Rodríguez, and Leandro Juan-Llácer, “MIMO Channel Sounder Based on Two Network Analyzers”, accepted for publication in IEEE Transactions on Instrumentation and Measurement.

[9] B. M. Donlan, David R. McKinstry and R. Michael Buehrer, “The UWB Indoor Channel: Large and Small Scale Modeling”, *IEEE* Transactions on Wireless Communications, vol. 5, no. 10, pp. 2863-2873, October 2006.